IONIC LIQUIDS AND HYPERBRANCHED POLYMERS – PROMISING NEW CLASSES OF SELECTIVE ENTRAINERS FOR EXTRACTIVE DISTILLATION

M. Seiler, C. Jork, T. Schneider, W. Arlt*

Technical University of Berlin, Institut fuer Verfahrenstechnik,
Fachgebiet Thermodynamik und Thermische Verfahrenstechnik,
Sekr. TK 7, Str. des 17. Juni 135, D-10623 Berlin, Germany

* Corresponding author. Tel.: ++49-30-31423977; fax: ++49-30-31422406.
Email address: W.Arlt@vt.tu-berlin.de

ABSTRACT

Ionic liquids (IL) and hyperbranched polymers (HyP) represent new classes of non-volatile selective solvents. By measuring vapor-liquid equilibria (VLE) of azeotropic and close boiling systems in the presence of ionic liquids or hyperbranched polymers, separation factors are derived and the potential of using IL and HyP as entrainer for extractive distillation is discussed. Exemplarily, the superiority of IL to conventional entrainers such as 1,2-ethanediol is pointed out by simulating extractive distillation processes for the separation of the azeotropic ethanol–water system using ASPEN PLUS®. The individual processes are energetically optimized and different unit operations for the regeneration of non-volatile entrainers are proposed. Both ionic liquids and hyperbranched polymers show remarkable selectivities, solubilities as well as low solution viscosities. They drastically increase the separation factor of many azeotropic and close boiling systems, which permits considerable improvements of processes such as extractive distillation.

Keywords:

Ionic liquids, hyperbranched polymers, extractive distillation, vapor-liquid equilibria, azeotropic mixtures, entrainer, separation factor

INTRODUCTION

Ionic Liquids (IL) and Hyperbranched Polymers (HyP) represent comparatively young species of substances, which – due to their unique structures and properties – are promising components for a wide variety of applications.

Ionic Liquids or Room Temperature Ionic Liquids[1] (RTIL) are substances, which entirely consist of ions. In contrast to conventional salts they have a melting point around ambient. Usually IL comprise an organic cation and an inorganic anion. Fig. 1 shows the ions that are often paired to build an ionic liquid.
Although the first IL was synthesised in 1914 [1] the research activities on this topic increased dramatically with the development of the first air- and moisture stable IL in 1992 [2] and with the commercial availability of IL in 1999 [3].
IL possess no effective vapor pressure, are relatively low viscous, are thermally stable up to 200°C, have a liquid range of about 300 K and are good solvents for a wide range of organic, inorganic and polymeric materials [4]. Moreover they are much less corrosive than conventional high melting salts [5]. Due to their properties IL are serious candidates for solvents in several industrial processes [6].
In synthetic chemistry, IL have been explored as solvents and catalysts. Many reactions performed in IL showed advantages with regard to enhanced reaction rates, improved selectivity or easier reuse of the catalysts [7] [5] [8]. IL are possible solvents for electrochemical applications and the use as electrolytes in batteries and photoelectrochemical devices was studied as well [9].
Studies about the thermal properties of a few IL provide some information regarding melting points, density, polarity and stability [10] [11] [7]. But there is no real understanding how the structure of an IL affects its physical properties. Until now, it cannot be predicted which IL are best for certain applications.
With the increasing comprehension on this topic one will be able to use the advantages of IL in comparison to volatile organic solvents. IL are truly designer solvents. By variation of the ions or the combination of ions approximately one trillion accessible IL can be formed (binary and ternary mixtures included) [12]. This large number of possible IL can be used to optimize production costs and IL-properties such as solubility, melting point, and thermal stability.
The use of IL in separation technology is promising [33] [34] but thermodynamic data are rare. There are only few investigations on vapor-liquid and liquid-liquid equilibria [13-15] including some investigations of extraction processes using IL [16-18].

Due to their unique structures and properties also highly branched, three dimensional polymers such as dendrimers [19] or hyperbranched polymers [20] attract increasing attention. Dendrimers are perfectly branched macromolecules, with a degree of branching (DB) of 1.0, which are only accessible by time consuming multi-step synthesis. An economically interesting alternative are the randomly branched hyperbranched polymers, which can easily be produced on large scale[2] by a one-pot polymerization of appropriate AB_2 monomers [21]. During the past 10 years a large body of interdisciplinary research on such polymers emerged and a wide variety of applications has been proposed [20] [22]. Most of these potential applications are based on peculiarities of the molecular interior and the remarkable thermal,

[1] sometimes simply called molten salts
[2] Companies such as *Perstorp Speciality Chemicals AB*, Sweden or *DSM*, Netherlands are already producing hyperbranched polymers known as BOLTORN and HYBRANE products on a ton-scale.

mechanical or solution properties, which can be tailored via the number and the nature of the functional groups.

The comprehension of the phase behavior is an essential prerequisite for contemporary polymer science and engineering. Phase separations often occur during the production and processing of polymers, either due to their necessity or owing to undesirable circumstances such as the incompatibility between polymers or an insufficient solvent power. Even though the experimental characterization of the miscibility behavior of hyperbranched polymers is an important requirement for a successful introduction of related applications to highly competitive markets, the understanding of the phase behavior of hyperbranched polymer solutions is still in its infancy.

An area of substantial industrial interest where hyperbranched polymers could be applied, is the field of thermal process engineering, an area which almost remained unconsidered in scientific discussions to date. Since the polarity of hyperbranched macromolecules can be adjusted by controlled functionalization of end groups, selective solvents – consisting of either pure hyperbranched polymers or fractions of hyperbranched additives – can be tailored [20] [21] [23]. Therefore, processes such as extractive distillation, solvent extraction, absorption, and emulsion liquid membranes appear as promising fields of applications [20] [21] [23]. Only recently, Seiler and Arlt revealed the potential of using hyperbranched polymers as selective solvents for the separation of azeotropic mixtures such as tetrahydrofuran–water by means of solvent extraction [24] [23] [35].

The remarkable solubility and selectivity, the low melt and solution viscosities as well as the high compatibility suggest, that hyperbranched polymers also can be used as selective entrainers for extractive distillation.

Therefore, this work aims to investigate the suitability of ionic liquids (IL) and hyperbranched polymers (HyP) as entrainers for extractive distillation. By measuring ternary vapor-liquid equilibria of azeotropic or close boiling systems in the presence of different amounts of IL or HyP, separation factors are determined. Exemplary for a successful separation of azeotropic mixtures, the extractive distillation process for the ethanol–water separation is modeled and energetically optimized by means of ASPEN PLUS®.

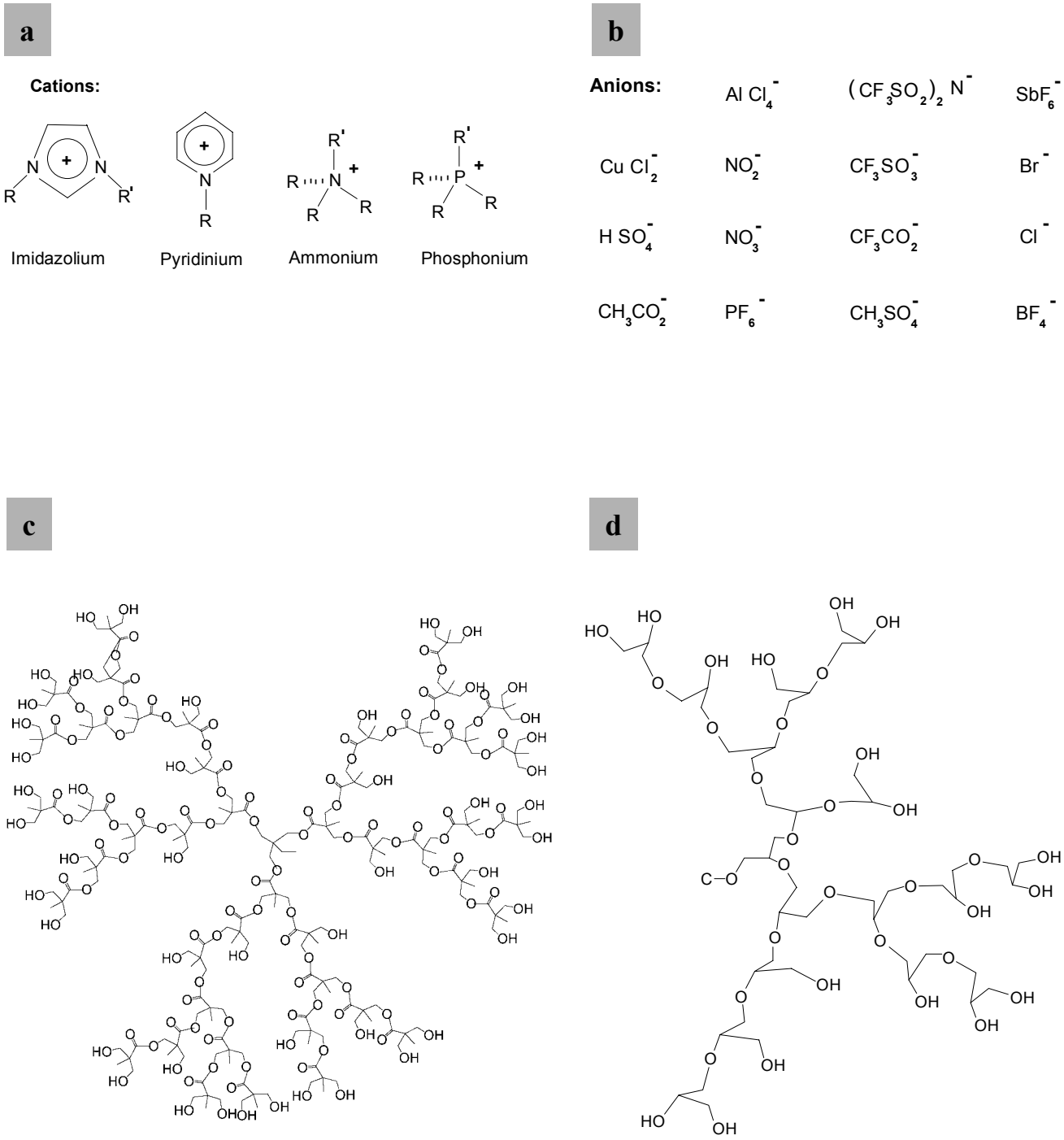

Fig.1. Structural details of the examined ionic liquids – consisting of anion/cation pairings – and hyperbranched polymers
Top: commonly used cations (a) and anions (b) for ionic liquids,
Bottom: hyperbranched aliphatic Boltorn-polyester (c), hyperbranched polyglycerol (d)

EXPERIMENTAL

Headspace - Gas Chromatography

"Headspace gas chromatography" (HSGC) [25] represents an experimental approach, which combines a headspace sampler and a gas chromatograph in order to determine the composition of a vapor phase. If the vapor phase is in equilibrium with a liquid or solid phase, vapor-liquid equilibria (VLE) or solid-vapor equilibria (SVE) can be measured and related thermodynamic information such as partial pressures, activity coefficients at finite and infinite dilution as well as interaction parameters can be obtained [21].

In this work HSGC was used for VLE measurements of the binary ethanol–water system and of ternary ethanol–water mixtures containing ionic liquids or hyperbranched polymers or 1,2-ethanediol. Furthermore, HSGC experiments were carried out for the systems acetone–methanol–IL and acetic acid–water–IL.

The chosen experimental approach is accurately described in [21].

Gas-liquid chromatography (GLC)

A pre-selection process of a variety of ionic liquids for their potential use as entrainer was carried out by determining the separation factor at infinite dilution. In case of a separation factor at infinite dilution, which differs from unity, vapor-liquid equilibria of azeotropic mixtures in the presence of potential entrainers were determined by means of headspace gas chromatography. Activity coefficients and separation factors at infinite dilution are measured by means of GLC as described in [26].

Materials

Ionic liquids

The ionic liquid 1-Ethyl-3-methylimidazolium tetrafluoroborate (in the following sections [EMIM][BF_4]) was provided by Solvent-Innovation (Germany). The purity was specified with ≥ 98%. This IL was dried several days at 110°C under vacuum to separate the IL from volatile byproducts and humidity.

Hyperbranched polymers

As hyperbranched macromolecular entrainers, hyperbranched polyglycerol samples and hyperbranched polyester samples (see Fig.1) of different molecular weight were used. Hyperbranched polyglycerol (sample PG1 and PG2, see below) was synthesized by slow addition of glycidol to a solution containing a partially deprotonated polyol core at 120 °C as described by Kautz et al. [27] and by Seiler et al. [21]. Perstorp Speciality Chemicals AB, Sweden (a company, which produces hyperbranched polymers on a ton-scale at a price of ca. 12 € / kg) provided aliphatic hyperbranched polyesters, known as the Boltorn family. The Boltorn samples used (*Boltorn H20* and *Boltorn H40*, see below) are hydroxyl functional hyperbranched polyesters, which are produced from polyalcohol cores and hydroxy acids. The hyperbranched structures are formed by polymerization of the particular core with 2,2-dimethylol proponic acid (Bis-MPA) [28]. The specifications of the hyperbranched polymer samples are listed below:

sample	molecular weight (g/mol)	number of OH-groups per macromolecule	M_w/M_n [a]	DB [b]
PG1	M_n = 1400 [b,c]	20 [c]	1.5	0.52
PG2	M_n = 4000 [b,c]	53 [c]	2.1	0.56
Boltorn H20	M_w = 2100 [*]	16	1.3	—
Boltorn H40	M_w = 5100 [*]	64	1.8	—

a) determined by SEC; **b)** calculated from ^{13}C-NMR spectra;
c) calculated from ^{1}H-NMR spectra; (*) see also [29]

Other materials

The solvents methanol, ethanol, acetone and 1,2-ethanediol with a purity >99.8 mol% and acetic acid with a purity >99 mol% were provided by Merck (Germany) and used as delivered. Distilled water was degassed and repeatedly filtered using 0.2 μm Millipore filter in order to remove dust.
Poly(ethylene glycol) PEG was obtained from Polysciences (Warrington, USA) with a molecular weight of M_w = 400 g/mol.

PROCESS SIMULATION AND OPTIMIZATION

Parameter Regressions

The simulation of processes employing ionic liquids and 1,2-ethanediol as entrainers are carried out using the ASPEN PLUS® Simulator (V. 10.01) from Aspen Technologies, Boston, MA. In a first step, several model parameters for the simulations need to be found. For this task, ASPEN PLUS® provides regression tools that fit parameters for a chosen model to measurement data.
For simulations of processes, in which the separation of mixtures is based on vapor-liquid equilibria (VLE), parameters for a g^E-model are needed that allow to calculate liquid phase activity coefficients. In this work, the common NRTL-model is chosen and the ionic liquid is treated like a non-dissociating component. If an ideal vapor phase is assumed, the vapor-liquid equilibria of the investigated systems can be calculated from the liquid concentrations, the activity coefficients and the vapor pressures of the pure substances.

Since the database of ASPEN PLUS® does not provide any pure component data of ionic liquids, additional model parameters for other properties of this component like vapor pressure and heat capacity need to be found.
In the following sections, parameter regressions for the pure component properties vapor pressure and heat capacity of the ionic liquid [EMIM][BF_4] as well as the regression for determining the NRTL-parameters of the ternary system ethanol–water–[EMIM][BF_4] are described.

Specific heat capacity of [EMIM][BF_4]

For describing the temperature dependence of the specific isobaric heat capacity c_p of a substance in ASPEN PLUS®, a polynomial approach is used:

$$c_p = C_1 + C_2T + C_3T^2 + C_4T^3 + C_5T^4, \quad (1)$$

where c_p is in J/(mol K) and T in °C.

Data for the heat capacity of [EMIM][BF_4] were determined using DSC (Differential Scanning Calorimetry) in a temperature range from 20°C to 130°C. Parameter regression yields the values for the five parameters listed in Tab.1:

Values calculated, using the parameters below, satisfactorily match the experimental data.

Tab. 1. Parameters for the heat capacity (Eq. 1) of [EMIM][BF_4] heat capacity in J/(mol K), temperature in °C

Parameter	Value
C_1	287.72
C_2	-0.273
C_3	3.70 E-03
C_4	-1.36 E-05
C_5	1.50 E-08

Vapor pressure of [EMIM][BF_4]

In ASPEN PLUS®, the temperature dependence of the vapor pressure is represented by an extended Antoine equation:

$$\ln p^{LV} = D_1 + \frac{D_2}{T + D_3} + D_4T + D_5 \ln T + D_6T^{D_7}, \quad (2)$$

where P^{LV} is in bar and T in °C. Because of the extremely low vapor pressure of ionic liquids, data for P^{LV} as a function of temperature are not easily accessed experimentally. On the other hand, setting P^{LV} = 0 bar over the entire temperature range, leads to numerical problems in the simulations. Therefore, a set of pseudo-data is used for the regression of parameters that provide extremely low values for the vapor pressure. Together with the NRTL-parameters presented in the next section, this approach leads to a good agreement between measured and calculated VLE-data. The parameter values are given in Tab. 2.

Tab. 2. Parameters for the vapor pressure of [EMIM][BF_4], (Eq. 2)
pressure in bar, temperature in °C.

Parameter	Value
D1	7.094
D2	-1323.897
D3	0
D4	0.005
D5	-3.512
D6	0
D7	0

g^E-model parameters for the system ethanol – water – [EMIM][BF_4]

Applying the NRTL-model to a ternary mixture means to predict liquid non-ideality in the ternary system from information about the three binary systems. For the system ethanol–water–[EMIM][BF_4], NRTL-parameters are needed for the binary systems ethanol–water, ethanol–[EMIM][BF_4] and water–[EMIM][BF_4]. While the parameters for the ethanol–water system are available from literature and also implemented in ASPEN PLUS®, the parameters for the other two systems have to be found by regression from experimental VLE-data.

The NRTL-model calculates activity coefficients from the parameters using the following equations:

$$\ln\gamma_i = \frac{\sum_j \tau_{ji} G_{ji} x_j}{\sum_k G_{ki} x_k} + \sum_j \frac{x_j G_{ij}}{\sum_k G_{kj} x_k}\left(\tau_{ij} - \frac{\sum_n x_n \tau_{nj} G_{nj}}{\sum_k G_{kj} x_k}\right) \qquad (3)$$

$$\text{with } \tau_{ij} = \frac{\Delta g_{ij}}{T}, \tau_{ii} = 0 \text{ and } G_{ij} = \exp(-\alpha_{ij}\tau_{ij}), G_{ii} = 1. \qquad (4)$$

Taking into consideration that $\alpha_{ij} = \alpha_{ji}$, only three parameters remain for each binary system.

Again, ASPEN PLUS® provides an extended version of the basic NRTL-model, which is supposed to reach a better representation of the temperature dependence of activity coefficients by calculating:

$$\tau_{ij} = a_{ij} + \frac{b_{ij}}{T} + e_{ij}\ln T + f_{ij} T \quad \text{and} \quad \alpha_{ij} = c_{ij} + d_{ij}\left(T - 273.15K\right). \qquad (5)$$

In this work, only parameters *a* to *c* are used, which keeps the model equation closer to the original NRTL-model.

The objective function for the regression of the NRTL-parameters is the equality of the fugacity for each component in both phases. With the assumption of an ideal vapor phase and at low to moderate pressures, the referring equation reads:

$$y_i P = x_i \gamma_i P_{0i}^{LV} . \quad (6)$$

For the component ionic liquid, this equation contains two values, which are close to zero: its vapor pressure and its concentration in the vapor phase. Therefore, to circumvent numerical problems, the parameter regression is not asked to fulfill the equation for the ionic liquid.
While the parameters for the binary system ethanol–water remained constant during the regression, the parameters for the systems ethanol–[EMIM][BF_4] and water–[EMIM][BF_4] were fitted to the experimental data for the ternary system in one single run. This approach was chosen because of a limited amount of [EMIM][BF_4]. The experimental data that were used for the regression can be found in Tab.6. The parameters that were found in the regression are presented in Tab. 3.

Tab. 3. NRTL-Parameters (Eq.3, Eq.5) for the system ethanol–water–[EMIM][BF_4] temperatures in K

Component i	**Ethanol**	**Ethanol**	**Water**
Component j	**Water**	**[EMIM][BF4]**	**[EMIM][BF4]**
$\mathbf{a_{ij}}$	-0.80	-5.01	103.91
$\mathbf{a_{ji}}$	3.46	-4.05	6.46
$\mathbf{b_{ij}}$	246.18	3580.69	-33052.31
$\mathbf{b_{ji}}$	-586.08	903.66	-3278.83
$\mathbf{c_{ij}}$	0.3	0.300	0.203

In Fig. 2 a comparison between measured VLE-data for different concentrations of [EMIM][BF_4] (see experimental VLE results in Tab. 6) and calculated values using Eq. (3) and (5) with the parameters from Tab. 3 is shown for a temperature of 90°C. On the abscissa, the molar concentration of ethanol is given as a pseudo-binary concentration as described in the chapter *RESULTS AND DISCUSSION*. As shown in Fig. 2, the calculated values are in good agreement with the measured data.

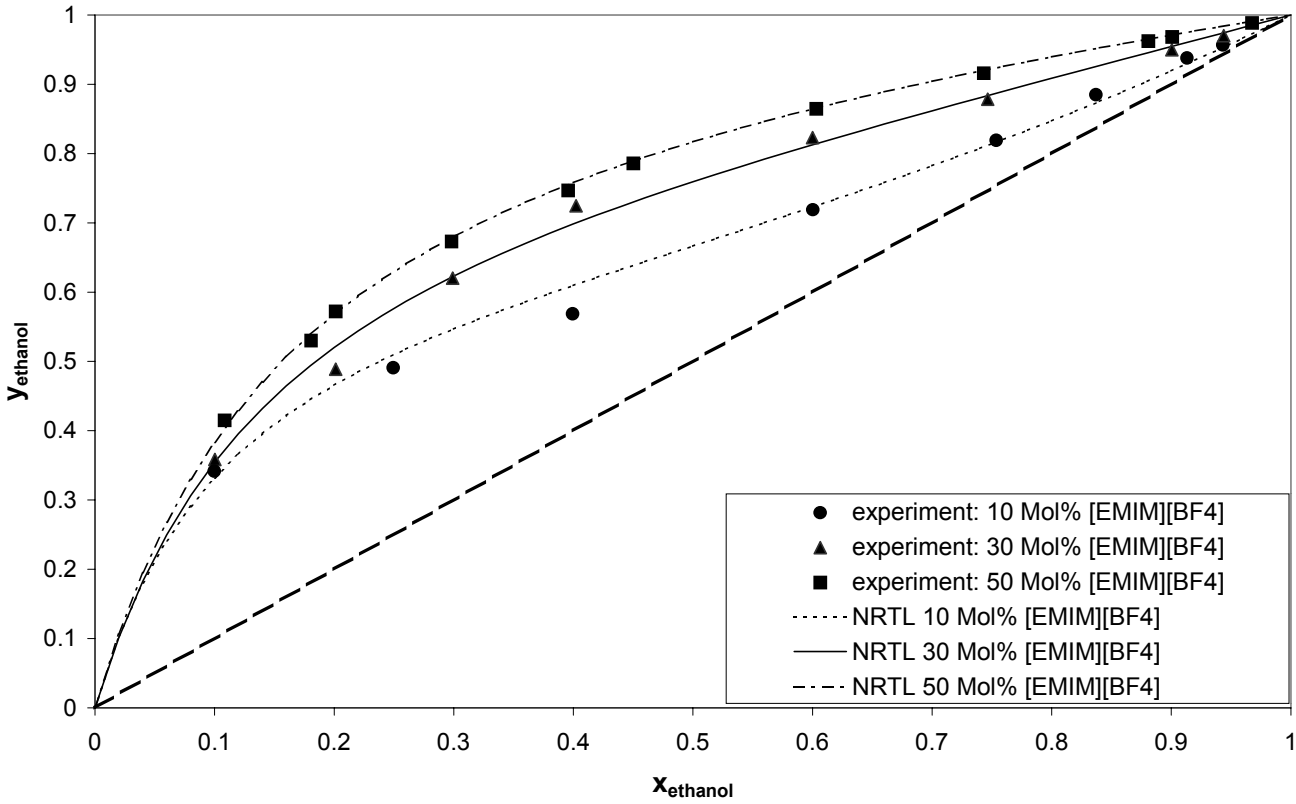

Fig. 2. Experimental VLE-data for the system ethanol–water–[EMIM][BF_4] and calculated VLE-curves using NRTL for 10 mol%, 30 mol% and 50 mol% IL at $T_{equilibrium}$ = 90 °C

g^E-model parameters for the system ethanol – water – 1,2-ethanediol

Pure component data for the component 1,2-ethanediol are available from the ASPEN PLUS® database and are used for the simulations. NRTL-parameters for the systems 1,2-ethanediol–water and 1,2-ethanediol–ethanol are also given in the database, but ternary VLE-data calculated from these parameters showed no adequate agreement with own experimental data. Therefore, a new set of parameters for these two systems was found by regression as described for the systems containing [EMIM][BF_4].

To ensure suitability of the latter parameters also for temperatures outside of the experimental data range (see Tab. 6 and Tab. 7), ternary equilibrium data, modeled by PC SAFT (Perturbed-Chain Statistical Associating Fluid Theory) equation of state, are used in addition to own experimental VLE results for the regression. The binary interaction parameters for PC SAFT and the parameters for the pure components ethanol, water and 1,2-ethanediol were determined by regression to published binary VLE-data and to pure component properties. The predicted ternary VLE was in good accordance with own experimental results.

The parameters that were found in the regression are presented in Tab. 4.

Tab. 4. NRTL-Parameters for the system ethanol–water–1,2-ethanediol, (Eq. 3 and Eq. 5); temperatures in K

Component i	Ethanol	Ethanol	Water
Component j	Water	1,2-Ethanediol	1,2-Ethanediol
a_{ij}	-0.80	0.97	-1.54
a_{ji}	3.46	-2.22	1.07
b_{ij}	246.18	-336.51	155.68
b_{ji}	-586.08	900.70	-19.50
c_{ij}	0.3	0.3	0.3

Simulation of the Extractive Distillation Process

For the simulation of the extractive distillation process a *separation task* is defined as follows: A stream of 200 kmol/h containing 70 mol% ethanol and 30 mol% water at a temperature of 76.8°C (i.e. saturated liquid) is to be separated in a way that yields a concentration of 99.8 mol% ethanol in the distillate and no more than 0.2 mol% ethanol in the bottom product. Furthermore, in order to allow an effective regeneration of the entrainer, the distillate stream should not contain more than $x_{entrainer}$ = 0.0001. Concentrations for the feed stream are chosen, assuming that a preconcentration of any feed with a lower concentration of ethanol would be used. For $x_{ethanol}$ < 0.7 the preconcentration can be easily carried out by distillation due to the high separation factors in the binary system ethanol–water. First simulations in an ASPEN PLUS® flowsheet are carried out defining only the extractive distillation column. Neither a preprocessing of the feed stream nor a recycling of the entrainer is regarded.

Optimization of the processes employing different entrainers

For a fair comparison between the effectiveness of the two different entrainers, both processes have to be optimized separately. Goal of the optimizations is to find a set of the following variables, which provides a minimum heat duty for the evaporator at the bottom of the column: amount of entrainer, reflux ratio as well as input stages for the feed and the entrainer stream, respectively. For both processes, the parameters listed in Tab. 5 are fixed.

The optimal input stage for the entrainer in an extractive distillation column is as close to the top stage as possible. This is, however, limited by the requirement of a low concentration of the entrainer in the distillate. Due to its low vapor pressure, the entrainer [EMIM][BF_4] can be added to the first stage below the condenser (stage 2) whereas the entrainer 1,2-ethanediol has to be added to stage 3 or 4, depending on the flowrate of entrainer. The remaining optimization parameters feed stage, reflux ratio and entrainer flowrate are evaluated as follows: For a given column of 30 theoretical stages and a given flowrate of the entrainer, the feed stage is varied in a reasonable range and the minimum reflux ratio that still allows to reach the concentrations specified in Tab.5 for each combination of entrainer flowrate and feed stage is found. The referring values are recorded together with the reboiler heat duties.

It is beyond dispute, that several reasonable optimization strategies can be chosen. Another procedure could be the specification of a constant entrainer mol fraction at a certain stage (for instance the feed stage) and to vary the reflux ratio of the column in such a way that the required purities are fulfilled. In this case, the reflux ratio would be an indicator for the effectiveness of an entrainer. Eventually, the results of this optimization, i. e. the reboiler heat duties, allow an energetical comparison of the distillation processes using 1,2-ethanediol and [EMIM][BF_4].
The authors are quite aware of the fact that the chosen optimization approach does not yield parameters for a completely optimized production scale process. It does, however, provide significant energetic data about the two different processes that allow a comparison between the different entrainers without discriminating either of them. Such a discrimination would be a comparison between an optimized and a non-optimized process. The results of the optimizations are given in the chapter *Simulation Results*.

Tab. 5. Fixed parameters for the optimization of the extractive distillation processes employing [EMIM][BF_4] and 1,2-ethanediol as entrainers

Feed		**Column**	
flowrate	200 kmol/h	operating pressure	1 bar
$x_{ethanol}$	0.7	theoretical stages	30
x_{water}	0.3	condenser	total, 3K subcooling
condition	saturated liquid	**Bottom product**	
Distillate		$x_{ethanol}$	$\leq$ 0.002
flowrate	140 kmol/h	**Entrainer**	
$x_{ethanol}$	$\geq$ 0.998		
$x_{entrainer}$	< 0.0001	temperature	75°C

RESULTS AND DISCUSSION

Vapor-Liquid Equilibria

In the following sections the influence of ionic liquids and hyperbranched polymers on vapor-liquid equilibria (VLE) of different azeotropic or close-boiling systems is described. To ensure accuracy of the headspace measurements, experimental results for the binary ethanol–water system were compared with high precision VLE literature data of Pemberton and Mash (see Fig. 3). Based on the assumption of an ideal vapor phase and NRTL-parameters from the DETHERM database [30], the NRTL-model allows for an accurate description of the binary ethanol–water VLE at 70°C and 90°C (see Fig. 3 and Fig. 4). Below, for the sake of clarity, the comparison between the ternary and the binary phase behavior will be done using the binary NRTL results instead of the experimental data. All phase diagrams are presented on a pseudo binary basis, i. e. the fraction of the binary ethanol–water solution amounts to $x_{ethanol+water} = 1 - x_{entrainer}$ for IL as an entrainer or $w_{ethanol+water} = 1 - w_{entrainer}$ for HyP as an entrainer and is splitted up according to the binary mol fractions plotted. Both entrainers represent non-volatile components with a vapor pressure of virtually 0 bar.

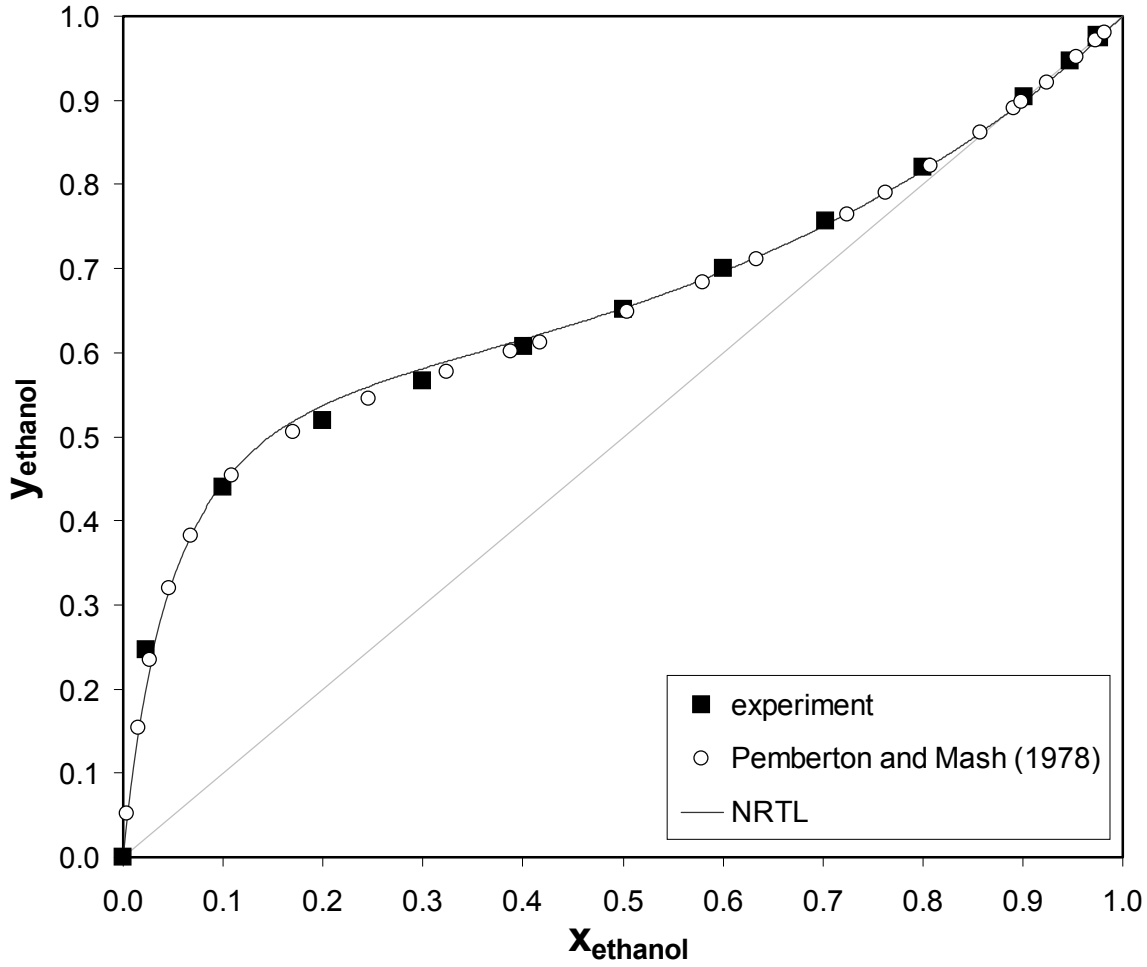

Fig. 3. Comparison of experimental results for the vapor-liquid equilibrium of ethanol–water with literature data of Pemberton and Mash [32]; System temperature $T_{equilibrium}$ = 90°C

Influence of [EMIM][BF_4] on the VLE of azeotropic and close-boiling systems

Ethanol – water – [EMIM][BF_4]

In Fig. 4 VLE-data for the binary system ethanol–water and the ternary system ethanol–water–[EMIM][BF_4] with a constant mol fraction of IL are depicted for a system temperature of 70°C. Fig. 4 illustrates that the addition of [EMIM][BF_4] to a binary ethanol–water mixture leads to an increase in the molar vapor fraction of ethanol. This is due to strong selective interactions between this IL and water molecules. In contrast to the binary ethanol–water mixture, these interactions decrease the water activity and thus result in an increased relative volatility of ethanol for mixtures containing more than $x_{ethanol} \approx 0.2$. With an amount of 10 mol% of [EMIM][BF_4] the system no longer exhibits azeotropic behavior. A further increase in [EMIM][BF_4]-concentration intensifies the effect of an increasing $y_{ethanol}$.

In Fig. 5 the influence of the ionic liquid [EMIM][BF_4] on the ethanol–water VLE is contrasted with the influence of the conventional entrainer 1,2-ethanediol for an equilibrium temperature of 90°C. In accordance to Fig. 4, also at 90°C a remarkable increase in $y_{ethanol}$ is observed for growing IL concentrations leading again to the elimination of the azeotropic phase behavior. Moreover, when comparing the two different entrainers for a concentration of 30 mol%, a clear superiority of [EMIM][BF_4] is obvious. Note, that the molar mass of the IL is considerably higher than the molar mass of ethanediol.

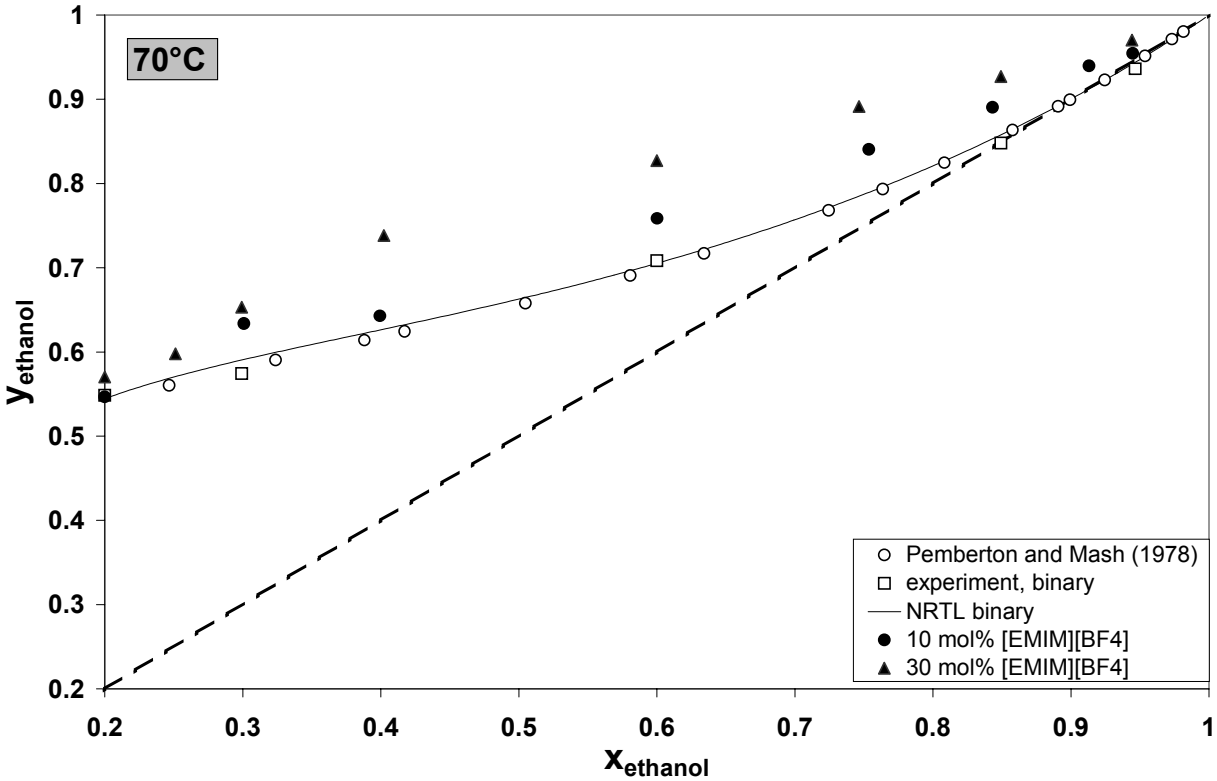

Fig. 4. Experimental VLE-data for the system ethanol–water–[EMIM][BF_4] for 0 mol%, 10 mol% and 30 mol% IL; calculated VLE-curves using NRTL and VLE literature data [32] for the binary ethanol–water system at $T_{equilibrium}$ = 70 °C

The ease of ethanol–water separation by means of distillation as well as the efficiency of an entrainer can be evaluated with the help of the separation factor and the separation efficiency. They are defined as follows:

separation factor

$$\alpha_{ethanol,water} = \frac{K_{ethanol}}{K_{water}} = \frac{\left(y_{ethanol} / x_{ethanol}\right)}{\left(y_{water} / x_{water}\right)} \tag{7}$$

separation efficiency

$$\beta = \frac{\left(\alpha_{ethanol,water}^{with\ entrainer}\right)_{ternary}}{\left(\alpha_{ethanol,water}^{without\ entrainer}\right)_{binary}} \tag{8}$$

Even though one sometimes can find definitions, which name Eq. (8) the selectivity of an entrainer, the authors use the latter term according to Eq. (9):

entrainer selectivity

$$S_{ethanol,water} = \left(\frac{\gamma_{ethanol}}{\gamma_{water}}\right)_{ternary} \tag{9}$$

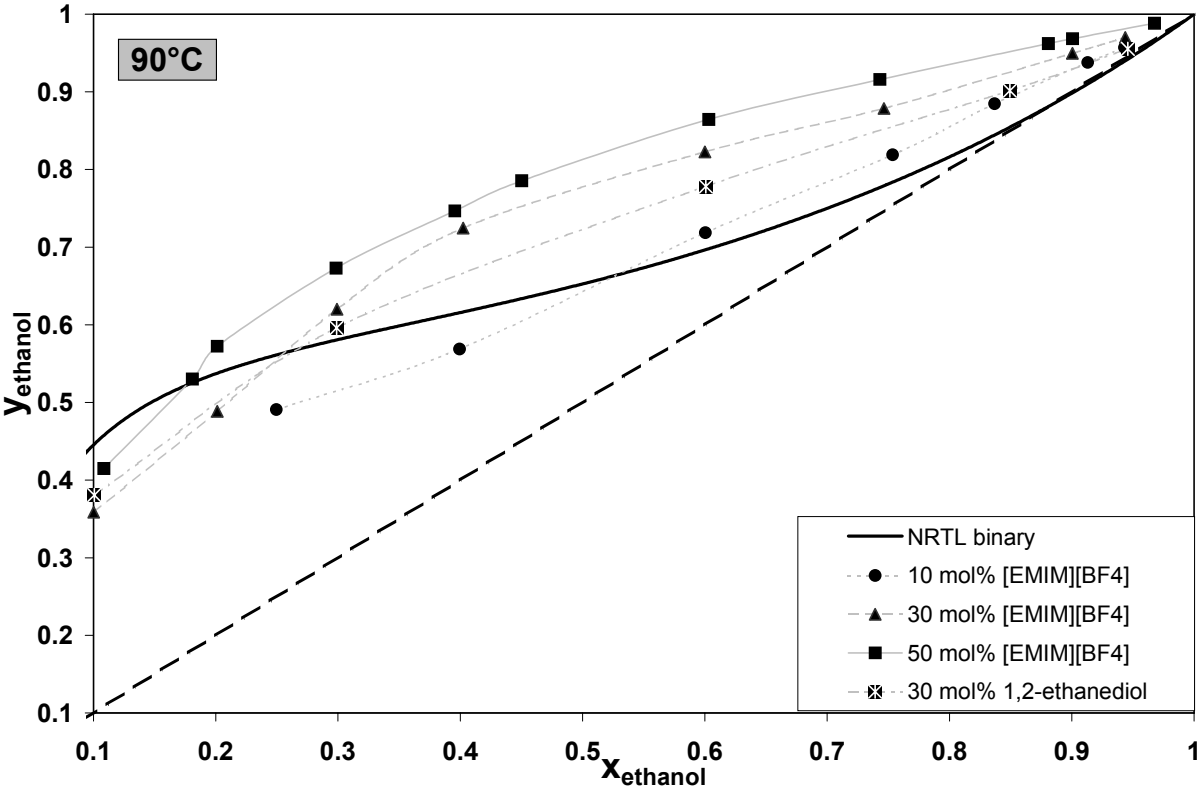

Fig. 5. Experimental VLE-data for the system ethanol–water–[EMIM][BF$_4$] for 10 mol%, 30 mol% and 50 mol% IL, experimental VLE-data for the system ethanol–water–1,2-ethanediol for 30 mol% 1,2-ethanediol and calculated VLE-curves using NRTL for the binary ethanol–water system, system temperature $T_{equilibrium}$ = 90 °C

In Fig. 6 and Fig. 7[3] the separation factor and the separation efficiency for the system ethanol–water–[EMIM][BF_4] are depicted for 70°C and 90°C. According to the presented VLE-results, for $x_{ethanol} > 0.2$, the separation factor $\alpha_{ethanol,water}$ increases considerably with increasing [EMIM][BF_4]-concentration. At the azeotropic point of the binary ethanol–water system for 70°C and 90°C, the separation factor $\alpha_{ethanol,water}$ of the ternary mixture is about 1.4 for 10 mol% [EMIM][BF_4], 2.1 for 30 mol% [EMIM][BF_4] and 3.3 for 50 mol% [EMIM][BF_4][4].

Analyzing the separation efficiency of [EMIM][BF_4] it becomes obvious that β passes through a maximum within the azeotropic ethanol–water region. Due to the remarkable selectivity of this ionic liquid towards water, both $\alpha_{ethanol,water}$ of the ternary system as well as the separation efficiency of [EMIM][BF_4] show a remarkable difference to the conventional entrainer 1,2-ethanediol and underline the potential of using ionic liquids in the field of extractive distillation.

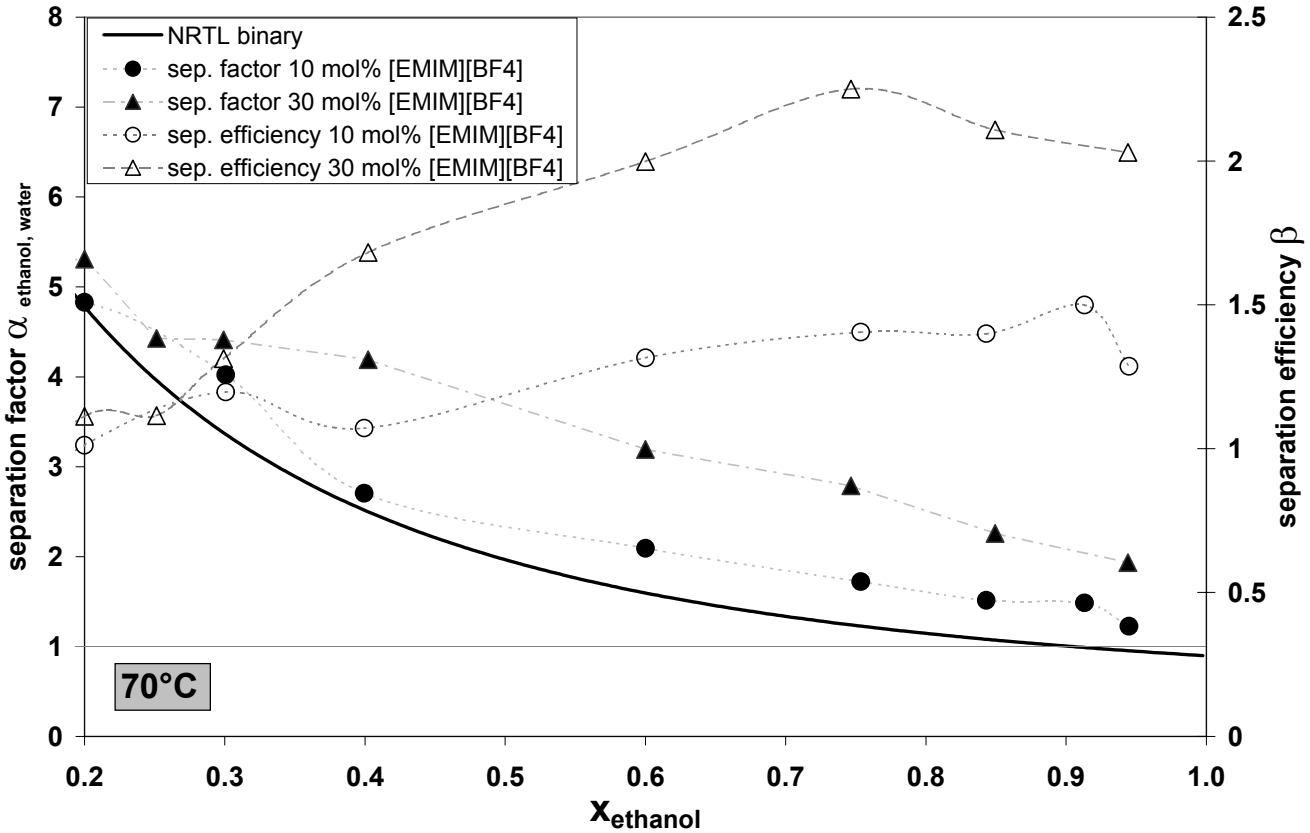

Fig. 6. Separation factor $\alpha_{ethanol–water}$ and the separation efficiency β of the system ethanol–water–[EMIM][BF_4] for 10 mol% and 30 mol% IL as well as the calculated separation factor $\alpha_{ethanol–water}$ for the system ethanol–water using NRTL at $T_{equilibrium}$ = 70 °C

[3] Please note that the line segments between the experimental points in the diagrams of this chapter are only a guide for the eyes and no calculated results.

[4] The VLE at a concentration of 50 mol% [EMIM][BF_4] was measured at 90°C only.

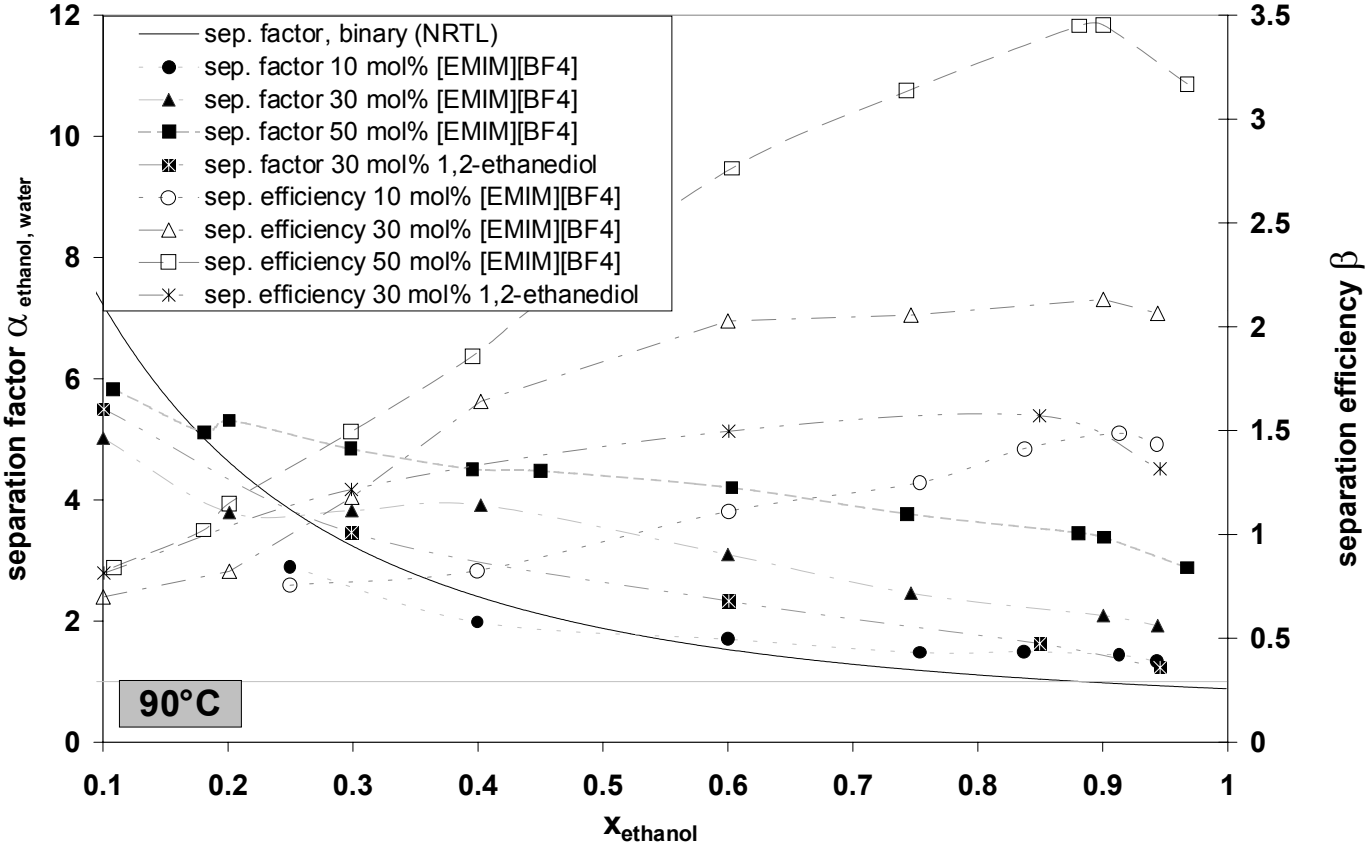

Fig. 7. Separation factor $\alpha_{ethanol-water}$ and the separation efficiency β of the system ethanol–water–[EMIM][BF$_4$] for 10 mol%, 30 mol% and 50 mol% IL, the separation factor $\alpha_{ethanol-water}$ and the separation efficiency β for the system ethanol–water–1,2-ethanediol for 30 mol% 1,2-ethanediol as well as the calculated separation factor $\alpha_{ethanol-water}$ for the system ethanol–water using NRTL at $T_{equilibrium}$ = 90 °C

Acetone – methanol – [EMIM][BF$_4$]

Apart from the system ethanol–water, IL are able to break the azeotropic behavior of a variety of azeotropic mixtures. This potential becomes evident when focusing on the IL [EMIM][BF$_4$] and its influence on other azeotropic or close boiling mixtures such as acetone–methanol or acetic acid–water.

Both the impact on the acetone–water VLE as well as the separation factor of [EMIM][BF$_4$] are depicted in Fig. 8 for a system temperature of 55°C. As for ethanol–water, only small concentrations of [EMIM][BF$_4$] are required (about 10 mol%) to surpass the azeotropic point of the acetone–methanol system. With increasing amount of IL the relative volatility of the lower boiling acetone increases, resulting in larger separation factors and separation efficiencies. It is worth mentioning, that even at the azeotropic point of the binary acetone–methanol system remarkable separation efficiencies of around 2 or larger can be achieved for $x_{[EMIM][BF4]} \geq 0.5$.

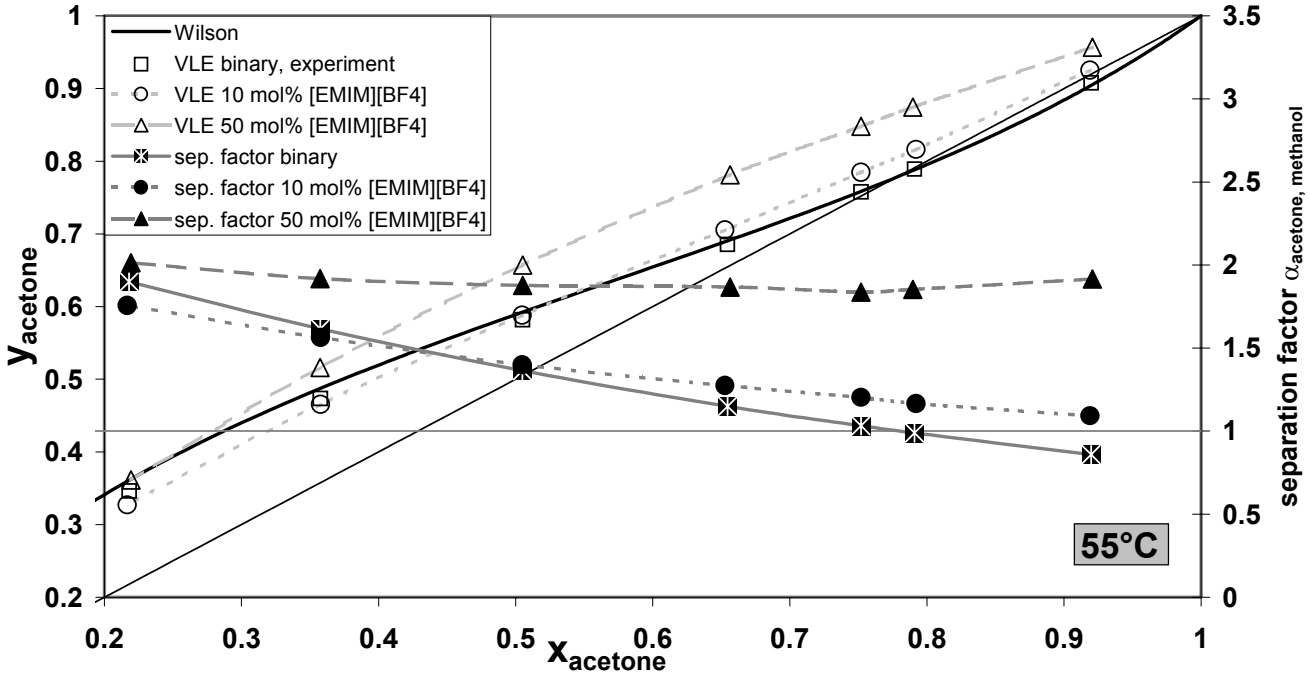

Fig. 8. Experimental VLE-data and the separation factor $\alpha_{acetone-methanol}$ of the system acetone–methanol–[EMIM][BF_4] for 0 mol%, 10 mol% and 50 mol% IL and the calculated VLE of the binary system acetone–water using the Wilson-model at $T_{equilibrium}$ = 55°C, (Wilson parameters based on published data of Freshwater and Pike, 1967)

Acetic acid – water – [EMIM][BF_4]

As can bee seen from Fig. 9, the separation factor of close boiling zeotropic systems like acetic acid–water can also be considerably increased by [EMIM][BF_4]-addition.

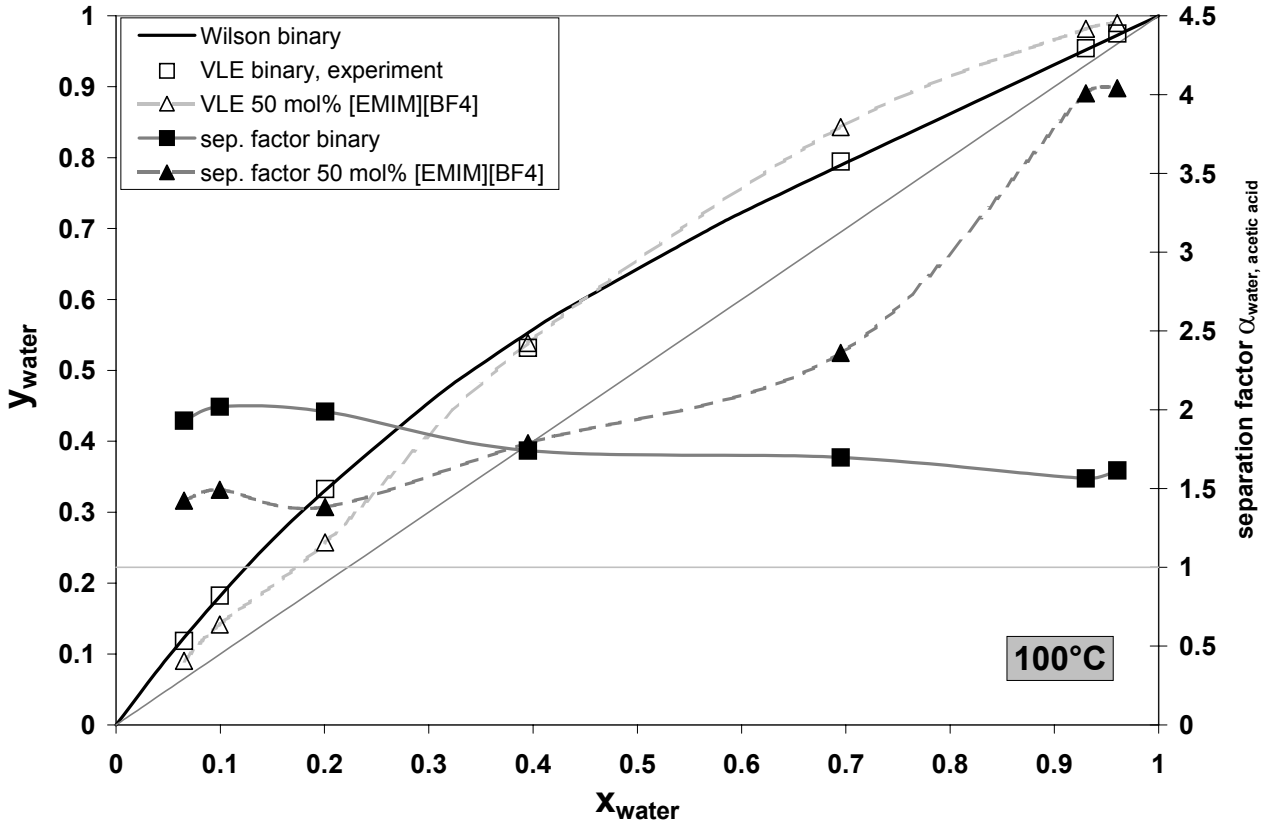

Fig. 9. Experimental VLE-data and the separation factor $\alpha_{water-acetic\ acid}$ of the system water – acetic acid – [EMIM][BF_4] for 0 mol% and 50 mol% IL and the calculated VLE of the binary system water – acetic acid using Wilson-model at $T_{equilibrium}$ = 100°C, (Wilson parameters based on published data of Acharya and Rao, 1947)

For 50 mol% of [EMIM][BF_4] and large pseudobinary water concentrations (x_{water} > 0.4), the attractive [EMIM][BF_4]–acetic acid interactions lead to a continuous increase in separation factor. For x_{water} ≈ 0.9 the separation factor of the ternary IL-containing system is more than twice as high as for the binary system (see Fig. 9). The described experimental VLE-results are summarized in Tab. 6.

Tab. 6. summary of the experimental binary and ternary VLE headspace results for systems using [EMIM][BF_4] as entrainer:

T = 70°C		T = 90°C		T = 90°C		T = 55°C		T = 100°C	
I		**II**		**II**		**III**		**IV**	
$x_{ethanol}$	$y_{ethanol}$	$x_{ethanol}$	$y_{ethanol}$	$x_{ethanol}$	$y_{ethanol}$	$x_{acetone}$	$y_{acetone}$	x_{water}	y_{water}
I a		**II a**		**II c**		**III a**		**IV a**	
0.200	0.549	0.250	0.491	0.045	0.213	0.218	0.346	0.065	0.119
0.299	0.574	0.399	0.569	0.108	0.415	0.357	0.474	0.100	0.182
0.600	0.708	0.600	0.719	0.181	0.530	0.505	0.582	0.200	0.333
0.849	0.848	0.754	0.819	0.201	0.572	0.655	0.685	0.395	0.532
0.946	0.936	0.837	0.885	0.298	0.673	0.752	0.758	0.695	0.795
		0.913	0.938	0.396	0.747	0.791	0.789	0.930	0.954
I b		0.943	0.957	0.450	0.786	0.920	0.908	0.960	0.975
0.100	0.342			0.603	0.865				
0.200	0.547	**II b**		0.743	0.916	**III b**		**IV b**	
0.301	0.634	0.100	0.359	0.881	0.962	0.217	0.327	0.065	0.090
0.399	0.643	0.201	0.489	0.901	0.968	0.358	0.466	0.100	0.142
0.600	0.759	0.299	0.620	0.968	0.989	0.505	0.588	0.200	0.257
0.754	0.840	0.402	0.725			0.653	0.706	0.395	0.539
0.843	0.891	0.600	0.823	**II d**		0.752	0.785	0.695	0.843
0.913	0.940	0.746	0.879	0.101	0.381	0.792	0.816	0.930	0.982
0.945	0.955	0.901	0.950	0.299	0.596	0.919	0.925	0.960	0.990
		0.944	0.970	0.601	0.778				
I c				0.849	0.902	**III c**			
0.100	0.367			0.946	0.955	0.219	0.361		
0.200	0.570					0.357	0.516		
0.251	0.598					0.505	0.657		
0.299	0.653					0.657	0.781		
0.402	0.738					0.752	0.848		
0.600	0.827					0.790	0.874		
0.746	0.891					0.921	0.957		
0.849	0.927								
0.944	0.970								

Ia : ethanol–water
Ib : ethanol–water–[EMIM][BF_4]; 10 mol% [EMIM][BF_4]
Ic: ethanol–water–[EMIM][BF_4]; 30 mol% [EMIM][BF_4]
IIa: ethanol–water–[EMIM][BF_4]; 10 mol% [EMIM][BF_4]
IIb: ethanol–water–[EMIM][BF_4]; 30 mol% [EMIM][BF_4]
IIc: ethanol–water–[EMIM][BF_4]; 50 mol% [EMIM][BF_4]
IId: ethanol–water–1,2-ethanediol; 30 mol% 1,2-ethanediol
IIIa: acetone–methanol
IIIb: acetone–methanol–[EMIM][BF_4]; 10 mol% [EMIM][BF_4]
IIIc: acetone–methanol–[EMIM][BF_4]; 50 mol% [EMIM][BF_4]
IVa: water–acetic acid
IVb: water–acetic acid–[EMIM][BF4]; 50 mol% [EMIM][BF4]

Ethanol – water – hyperbranched polymers

Due to their large number of functional groups, hydroxyl functional hyperbranched polymers show a remarkable solubility in polar solvents such as water or ethanol. As recently described in [21] for these polymer solutions, the extent of inter- and intramolecular hydrogen bond formation is the dominating impact factor on solvent activity and therefore determines partition coefficients and separation factors. Since the synthesis of hyperbranched polymers allows for the tailoring of properties such as solubility, solution viscosity, selectivity and capacity, the authors analyzed the potential of using hyperbranched polymers as entrainer for the separation of azeotropic mixtures.

Fig. 10 and Fig. 11 as well as Tab. 7 show experimental VLE-results for ternary ethanol–water mixtures containing different kinds of hyperbranched polymers: hyperbranched polyglycerols (samples PG1 and PG2) and hyperbranched aliphatic polyesters (sample *Boltorn H20* and *Boltorn H40*). The influence of hyperbranched polymers on VLE and separation factor of the ethanol–water system is compared to the influence of the conventional entrainer 1,2-ethanediol and the linear polymer polyethylene glycol (PEG).

As can be seen from Fig. 10 and Fig. 11, for $w_{polymer}$ < 20 ma% the respective polymers do not have a strong impact on the solvent activities. For this range of polymer concentration, the interactions between polymer and water and polymer and ethanol respectively, are of the same intensity. Moreover, due to good polymer solubility, intermolecular solvent-polymer interactions dominate over polymer-polymer and intramolecular polymer interactions. Hence, below $w_{polymer}$ = 20 ma%, both kinds of hyperbranched polymers – the hyperbranched polyglycerol samples PG1 and PG2 as well as the hyperbranched aliphatic polyesters *Boltorn H20* and *Boltorn H40* – do not affect the vapor-liquid equilibrium and the separation factor of the ethanol–water system at 90°C.

For polymer concentrations above 20 ma% and $x_{ethanol}$ > 0.2, the extent of hydrogen bond formation between the individual hyperbranched polymer and water increases, leading to a larger molar vapor fraction of ethanol in contrast to the binary ethanol–water VLE (see Fig. 10 and Fig. 11). As far as the hyperbranched polymer samples PG1, PG2 and *Boltorn H20* are concerned, a polymer concentration larger than $w_{polymer}$ = 40 ma% results in breaking the azeotrope of the ethanol–water system. At $x_{ethanol}$ = 0.9, the azeotropic concentration of the binary ethanol–water system at 90°C, the ethanol concentration in the vapor phase $y_{ethanol}$ and hence the separation factor $\alpha_{ethanol,water}$ increases with increasing polymer concentration until the maximum amount of polymer is solved and/or the maximum number of polymer–water hydrogen bonds is formed.

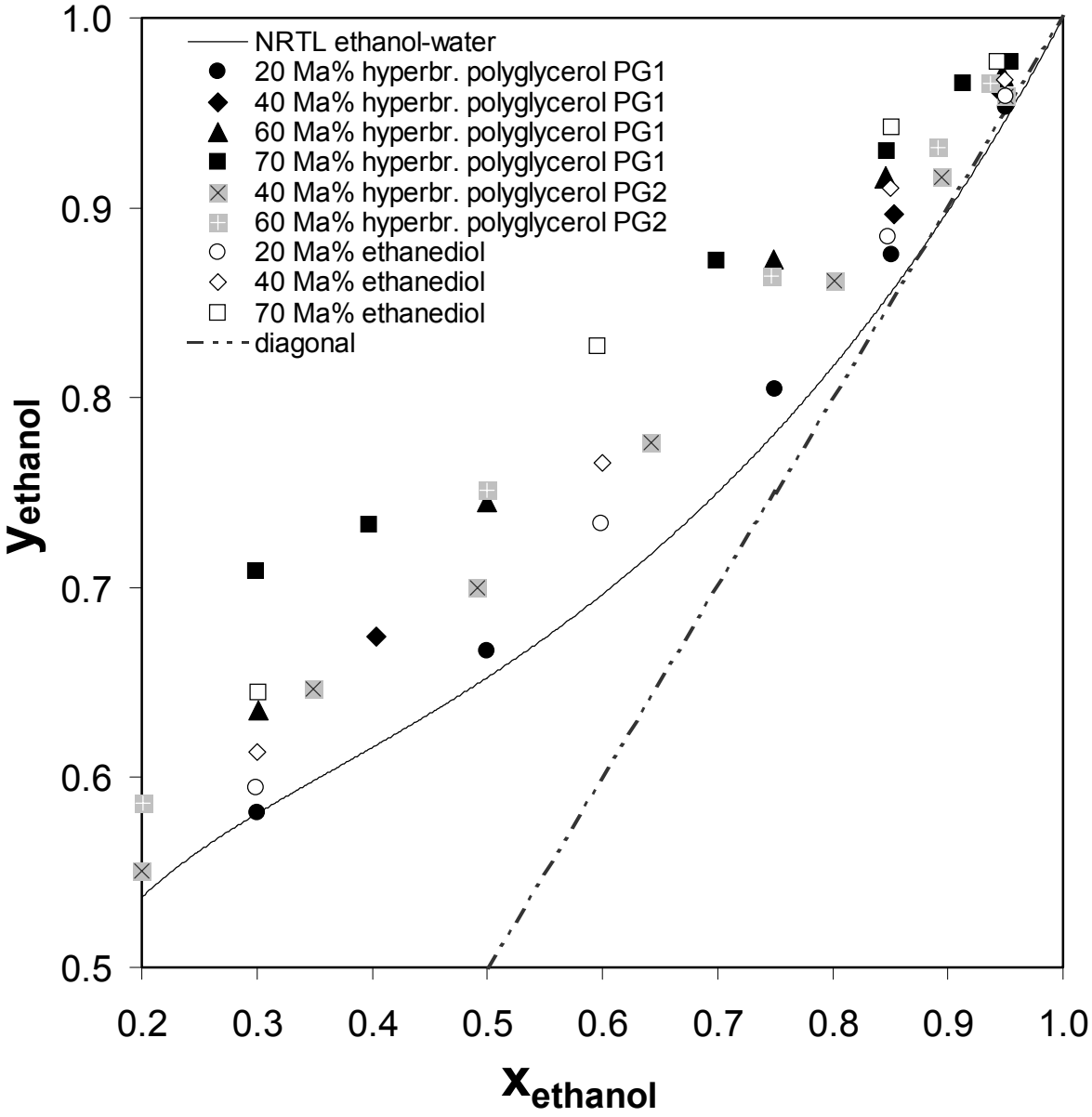

Fig. 10. Experimental VLE-results for the system hyperbranched polyglycerol–ethanol–water and 1,2-ethanediol–ethanol–water for different polymer and 1,2-ethanediol concentrations at $T_{equilibrium}$ = 90 °C;
hyperbranched polyglycerol PG1: M_n=1400 g/mol, M_w/M_n =1.5;
hyperbranched polyglycerol PG2: M_n=4000 g/mol, M_w/M_n =2.1;

When contrasting the hyperbranched polyglycerol structures with the hyperbranched *Boltorn* polyesters of the same molecular weight it becomes evident that the samples PG1 and *Boltorn H20* and PG2 and *Boltorn H40* respectively, have a comparable number of hydroxyl groups per molecule. Nevertheless, at the azeotropic point of the ethanol–water system, hyperbranched polyglycerol shows almost complete miscibility whereas the solubility of the individual aliphatic polyester is restricted to about 63 ma% of polymer (62 ma% for *Boltorn H20* and 65 ma% for *Boltorn H40*). Both the solubility behavior of the individual polymer as well as the number of functional groups per macromolecule, seem to determine the separation factor of the respective ternary system. Based on Fig. 10 and Fig. 11, Fig. 12 shows the separation factor $\alpha_{ethanol,water}$ as well as the separation efficiency β in dependence of the pseudo-binary liquid ethanol mol fraction. For ethanol-rich solutions, the highest separation factor and separation efficiency is achieved at a polyglycerol concentration of approximately

$w_{polym.,PG1} \approx 70$ ma%. For this concentration, a decrease in temperature from 90°C to 70°C results in considerable increase of $\alpha_{ethanol,water}$ and β. Because of the remarkable solubility of the hyperbranched polyglycerol sample PG1, a further increase in polymer concentration is still possible. However, for $x_{ethanol} > 0.9$ and $w_{polymer,PG1} > 0.6$, a lack of water molecules – the preferred hydrogen bonding partner of hyperbranched polyglycerol – prevails, leading to a constant separation factor at 90°C (see [21]). Since, for $0.6 < w_{polymer,PG1} < 0.7$ and large ethanol concentrations, most of the water molecules are already hydrogen bonded to a hyperbranched macromolecule, a further increase in polymer (PG1) concentration most likely results in a rising number of hydrogen bonds between ethanol and polymer and thus in a decrease in PG1-selectivity for water.

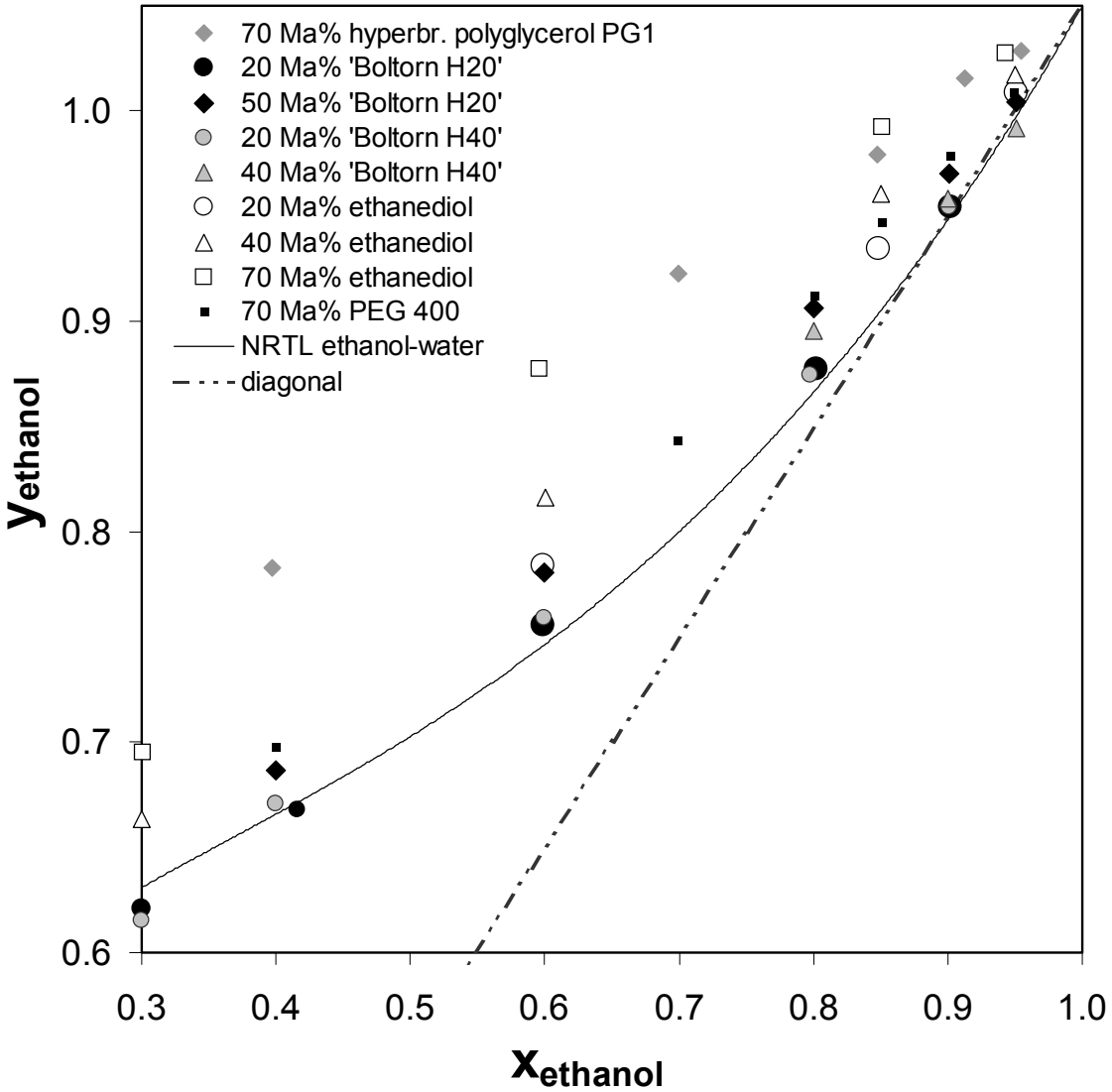

Fig. 11. Experimental VLE results for the system hyperbranched polyester–ethanol–water and 1,2-ethanediol–ethanol–water for different polymer and ethanediol concentrations at $T_{equilibrium}$ = 90°C;
hyperbranched aliphatic polyester 'Boltorn H20': M_w=2100 g/mol, M_w/M_n=1.3
hyperbranched aliphatic polyester 'Boltorn H40': M_w=5100 g/mol, M_w/M_n=1.8

From Fig. 12 it can be concluded that the influence of the conventional entrainer 1,2-ethanediol and hyperbranched polyglycerol PG1 on the separation factor $\alpha_{ethanol,water}$ are of the same magnitude, whereas the hyperbranched aliphatic *Boltorn* samples as well as the alleged polymeric entrainer poly(ethylene glycol)[5] exhibit a rather modest effect on the separation factor with only very limited use within the field of extractive distillation.

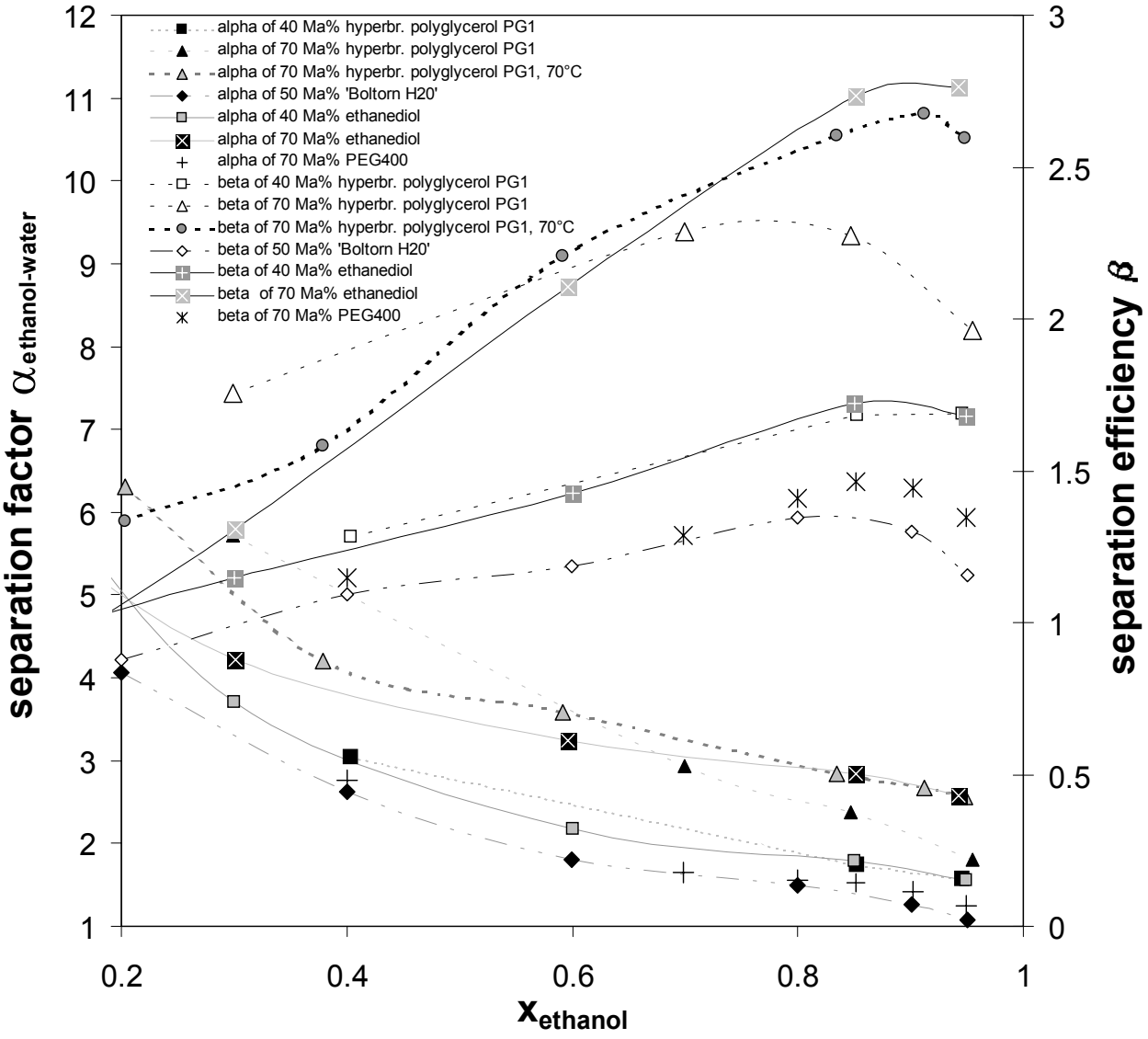

Fig. 12. Separation factors and separation efficiencies for ethanol–water mixtures containing hyperbranched polyglycerol, hyperbranched polyester, poly(ethylene glycol) or 1,2-ethanediol; $T_{equilibrium}$ = 90°C unless otherwise indicated in the legend

[5] Al-Amer suggested poly(ethylene glycol) as promising polymeric entrainer for the ethanol–water separation by extractive distillation [31].

Advantages of using hyperbranched polyglycerol instead of 1,2-ethanediol as entrainer might become evident when focusing at possible, competing operation steps for the entrainer regeneration. In case of the non-volatile entrainer hyperbranched polyglycerol, a variety of separation steps can be used for the entrainer–water separation.
Especially countercurrent distillation by means of a stripping column, evaporation by means of a thin film evaporator, drying by means of a thin-film evaporation dryer or the simple crystallization of water might result in an improved azeotropic separation process, which eventually is superior to conventional extractive distillation processes (see also chapter *Entrainer Regeneration*).

Tab. 7. experimental VLE result summary for the systems listed below:

T = 90 °C		T = 70 °C		T = 90 °C		T = 90 °C		T = 90 °C		T = 90 °C		T = 90 °C		T = 90°C	
I		**II**		**III**		**IV**		**V**		**VI**		**VII**		**VIII**	
$x_{ethanol}$	$y_{ethanol}$	$x_{ethanol}$	$y_{ethanol}$	$x_{ethanol}$	$y_{ethanol}$	$x_{ethanol}$	$y_{ethanol}$	$x_{ethanol}$	$y_{ethanol}$	$x_{ethanol}$	$y_{ethanol}$	$x_{ethanol}$	$y_{ethanol}$	$x_{ethanol}$	$y_{ethanol}$
				III a		**IV a**		**V a**		**VI a**		**VII a**			
0.0230	0.2458	0.2030	0.6164	0.1001	0.4593	0.0200	0.2177	0.1001	0.4485	0.1999	0.5225	0.0999	0.4324	0.6989	0.7936
0.1000	0.4394	0.3791	0.7197	0.2998	0.5817	0.0501	0.3635	0.2995	0.5949	0.2998	0.5708	0.1996	0.5172	0.4001	0.648
0.1998	0.5195	0.5910	0.838	0.4996	0.6667	0.2001	0.5510	0.5989	0.7337	0.4160	0.6179	0.3000	0.5653	0.8002	0.8622
0.3002	0.5665	0.8351	0.935	0.7503	0.8042	0.3493	0.6466	0.8482	0.8845	0.5987	0.7054	0.3999	0.6207	0.8511	0.8967
0.4002	0.6078	0.9013	0.9682	0.8510	0.8755	0.4914	0.7000	0.9507	0.9588	0.8018	0.8274	0.6001	0.709	0.9018	0.9285
0.5010	0.6521	0.9480	0.9791	0.9506	0.9531	0.6420	0.7763			0.9021	0.9046	0.7982	0.8246	0.9495	0.9587
0.6005	0.7005					0.8014	0.8614	**V b**				0.9014	0.9046		
0.7035	0.7564			**III b**		0.8943	0.9160	0.1005	0.4314	**VI b**					
0.8004	0.8210			0.4040	0.6739	0.9503	0.9588	0.3000	0.6135	0.2001	0.5043	**VII b**			
0.9011	0.9042			0.8531	0.9101			0.6005	0.7659	0.3999	0.6367	0.7999	0.8454		
0.9476	0.9473			0.9460	0.9651	**IV b**		0.8504	0.9107	0.5996	0.7306	0.9002	0.9081		
0.9763	0.9753					0.2008	0.5865	0.9498	0.9672	0.8002	0.8565	0.9506	0.9417		
				III c		0.4998	0.7511			0.9010	0.9204				
				0.1004	0.4451	0.7465	0.8638	**V c**		0.9509	0.9541				
				0.3012	0.6353	0.8914	0.9315	0.0996	0.3979						
				0.4997	0.7448	0.9375	0.9653	0.3010	0.6450						
				0.7487	0.8730			0.5959	0.8273						
				0.8464	0.9162			0.8512	0.9420						
				0.9476	0.9701			0.9428	0.9771						
				III d											
				0.2988	0.7088										
				0.6993	0.8724										
				0.8473	0.9295										
				0.9549	0.9746										

I: ethanol–water;
II: ethanol–water–PG1, 70 Ma% PG1
III: ethanol–water–PG1, III a: 20 Ma% PG1, III b: 40 Ma% PG1, III c: 60 Ma% PG1, IIId: 70 Ma% PG1
IV: ethanol–water–PG2, IV a: 40 Ma% PG2, IV b: 60 Ma% PG2
V: ethanol–water–ethanediol(ED), V a: 20 Ma% ED, V b: 40 Ma% ED, V c: 70 Ma% ED
VI: ethanol–water–'Boltorn H20', VI a: 20 Ma% 'Boltorn H20', VI b: 50 Ma% 'Boltorn H20'
VII: ethanol–water–'Boltorn H40', VII a: 20 Ma% 'Boltorn H40', VII b: 50 Ma% 'Boltorn H40'
VIII: ethanol–water–PEG, 70 Ma% PEG
***PG**: hyperbranched polyglycerol samples as specified above, **ED**: 1,2-ethanediol,*
***PEG**: Poly(ethylene glycol)*

Therefore, it can be concluded that hyperbranched polyglycerol represent a promising entrainer or entrainer additive for the ethanol–water separation by means of extractive distillation.

Simulation Results

The results of the optimization described in the section *Simulation of the Extractive Distillation Process* are presented in this chapter. Fig. 13 shows the reboiler heat duty as well as the minimum reflux ratio for different flowrates of the referring entrainer[6].

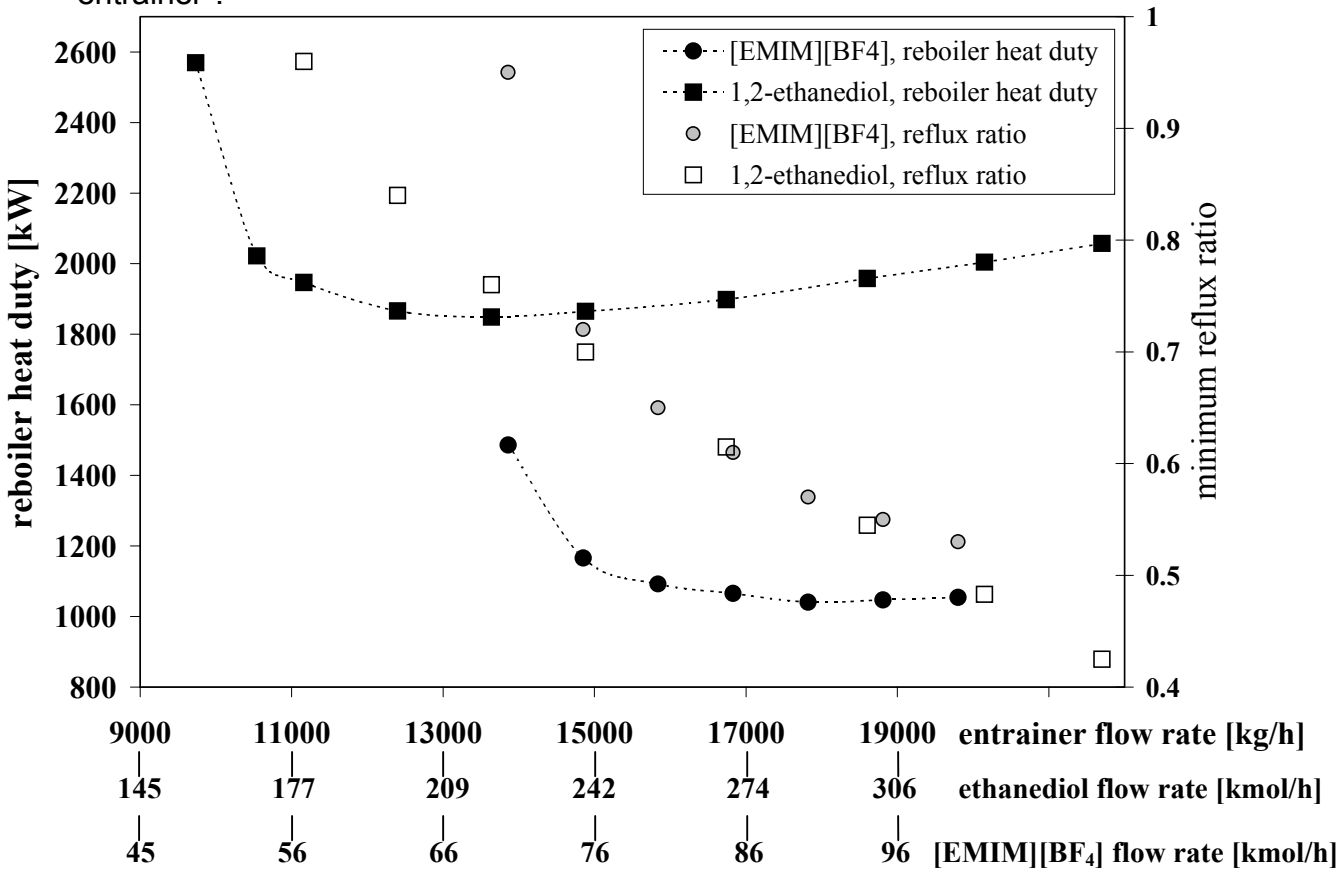

Fig. 13. Comparison of reboiler heat duty versus entrainer flowrate between the optimized extractive distillation processes using [EMIM][BF_4] and 1,2-ethanediol as entrainer, respectively.

As can be seen from Fig.13, an increase of the entrainer flowrate allows a reduction of the reflux ratio. On the other hand, an increase of the amount of entrainer is followed by an additional heat requirement for the heating of the entrainer from 75°C (temperature at input stage) to the temperature of the bottom of the column. Therefore, the reboiler duty passes through a minimum for a certain entrainer flowrate.

While it is tempting to choose this minimum as the optimal configuration for the process, the regeneration of the entrainer as another energy consuming process step also has to be taken into consideration. Therefore, the optimal entrainer flowrate is chosen as the flowrate for which further addition of entrainer does not lead to a significant reduction of the reboiler duty in the extractive distillation column. The data for the optimal configurations of the respective extractive distillation columns are given in Tab. 8.

---

[6] The mass-referred flow rate in Fig. 13 is related to both entrainers, i. e. [EMIM][BF_4] and 1,2-ethanediol.

Tab. 8. Parameters for the optimized extractive distillation column

entrainer	[EMIM][BF_4]	1,2-ethanediol
entrainer flowrate [kmol/h]	80	200
entrainer flowrate [kg/h]	15838	12414
reflux ratio	0.65	0.84
boilup ratio	0.73	0.51
reboiler heat duty [kW]	1092	1866
condenser heat duty [kW]	2587	2788
feed stage	23	23
entrainer stage	2	4
distillate [kmol/h]	140	140
$x_{ethanol}$	0.9981	0.9980
x_{water}	0.0019	0.0020
$x_{entrainer}$	< 0.000001	< 0.00001
bottom product [kmol/h]	140	260
$x_{ethanol}$	0.0019	0.0011
x_{water}	0.4267	0.2297
$x_{entrainer}$	0.5714	0.7692

While the process employing the ionic liquid uses much less entrainer expressed on a molecular basis, the flowrates on a mass basis are in the same order of magnitude. This is due to the higher molar mass of the ionic liquid (198 g/mol) compared to 1,2-ethanediol (62 g/mol).
The most interesting difference is the significantly higher energy consumption of the extractive distillation column employing 1,2-ethanediol compared to the column with IL, which needs less than 60% of the energy. In both processes the specifications for the outlet streams are satisfied. While the optimal feed stage is the same for both processes, the entrainer stage in the process employing 1,2-ethanediol can not be above stage 4 as this would lead to an unacceptable concentration of entrainer in the distillate.

Entrainer Regeneration
The entrainer recovery in a conventional extractive distillation process is mostly carried out using a second countercurrent distillation column. In contrast to this conventional process, the regeneration of non-volatile entrainers such as ionic liquids or hyperbranched polymers allows the use of other unit operations.
As described below, both ionic liquids and hyperbranched polymers can be separated from low boiling substances like water by means of a stripping column, appropriate thin-film evaporators, dryers or crystallizers when applicable.

Conventional distillation for the separation of a binary mixture consisting of a non-volatile entrainer and a volatile component is not eligible, since the non-volatility of a component would lead to a brake down of the columns' counterflow. A possibility to circumvent this problem is the operation of a stripping column (charge reflux fractionator) without rectifying section and reflux. At the bottom of the stripper, heated inert gas can be fed into and guided through the column in countercurrent to the entrainer-rich feed, resulting in a concentrated entrainer-bottom product.
Thin-film evaporators represent another alternative for an effective, thermally gentle and continuous recycling of a non-volatile entrainer. For ionic liquid recovery, falling-film evaporators can be used, whereas, for the higher viscous hyperbranched polymers, rotary thin-film evaporators appear to be suitable. Although the hyperbranched polymer melts show comparatively low viscosities, it might be advantageous to install a refuse worm at the rotor end of the thin-film evaporator such as those used for the stripping of epoxy resins or the degassing of polyolefins.
Ionic liquids and hyperbranched polymers can also be recycled by convection drying, using a spray dryer, a thin-film evaporation dryer or a belt dryer. Does the non-volatile entrainer show the lowest crystallization or glass transition temperature of all mixture components, crystallization by means of a cooling crystallizer, a classifying crystallizer or a spray crystallizer would also be conceivable.

The recovery options described for a non-volatile entrainer represent competing unit operations, which have to be thoroughly assessed according to their investment and operation costs. A comparison with conventional separation processes for azeotropic mixtures (especially with the two pressure distillation) shows, that the remarkable separation efficiencies of ionic liquids and hyperbranched polymers as well as the variety of energetically promising recycling options for the entrainer offer a considerable potential for process optimizations and cost savings.
Regarding the optimized extractive distillation using 1,2-ethanediol, an entrainer regeneration by means of distillation requires more than 1090 kW. This heat duty represents the reboiler heat duty of a packed column, equipped with the regular packing type *Mellapak 250.Y* and operated under vacuum (P = 100 mbar) with 14 stages and a reflux ratio of 1.0. To ensure appropriate loading limits (especially an adequate distance to the diswetting limit) a maximum F-factor of 2.5 $Pa^{0.5}$ and a minimum liquid load of 1.0 $m^3/(m^2\ h)$ were chosen as underlying operating criteria[7]. The required purities for the entrainer regeneration were specified as follows:

> 99.95 mol% for the 1,2-ethanediol bottom product,

< 0.05 mol% for the 1,2-ethanediol fraction in the distillate.

Hence – based on the results of the optimization above (see Tab. 8) – it can be concluded:
if the regeneration unit of the extractive distillation process using [EMIM][BF_4] as entrainer would be operated with a heat demand of about 1864 kW[8], the two complete processes including entrainer regeneration would become energetically identical. In other words, if a regeneration unit is fed with the bottom product of the

[7] For these operating criteria the diameter of the regeneration column amounts to 1.2 m and the Height Equivalent to one Theoretical Plate (HETP) corresponds to 0.4. The feed for the 1,2-ethanediol regeneration is given by the bottom product of the extractive distillation column as specified in Tab.8.

[8] 1864 kW = [main column reboiler heat duty of ethanediol process] **+** [heat duty of ethanediol regeneration] **-** [main column reboiler heat duty of EMIM BF_4 process]

[EMIM][BF_4]-column as specified in Tab. 8 and could be operated with a heat demand smaller than 1864 kW, the entire extractive distillation process using [EMIM][BF_4] as entrainer would be energetically superior to the conventional ethanediol process. Since, for the [EMIM][BF_4]-regeneration a variety of competing operations are available and the molar flowrate amounts to 50% of the feed for the ethanediol-regeneration, the prospects of realizing such a process with energetic superiority are very promising.

CONCLUSIONS AND FUTURE WORK

Ionic Liquids (IL) and hyperbranched polymers (HyP) represent promising classes of entrainers or entrainer additives for extractive distillation [33] [34] [23]. Both classes are non-volatile, highly selective solvents, whose properties can be tailored according to the aspired application. In this work the potential of ionic liquids and hyperbranched polymers for the field of extractive distillation is discussed by measuring ternary (IL- and HyP-containing) vapor-liquid equilibria of a selection of azeotropic and close-boiling systems, by contrasting the separation factor of the binary and the ternary system and by determining the separation efficiencies of the ionic liquid [EMIM][BF_4] and different hyperbranched polymers such as hyperbranched polyglycerols and aliphatic hyperbranched polyesters. The IL [EMIM][BF_4] as well as the hyperbranched polyglycerol sample PG1 exhibit remarkable separation efficiencies. Regarding the azeotropic system ethanol–water both representatives easily break the azeotropic phase behavior by interacting selectively with water. For $x_{ethanol} > 0.3$, a considerable increase of the separation factor $\alpha_{ethanol,water}$ was observed when adding [EMIM][BF_4] or hyperbranched polyglycerol to the ethanol–water system. In the case of [EMIM][BF_4] this increase proved to be larger than that of the conventional entrainer 1,2-ethanediol and in the case of the hyperbranched polyglycerol PG1 the increase was of the same magnitude. To underline the enormous potential of ionic liquids and hyperbranched polymers for the field of extractive distillation, ASPEN PLUS® simulations and optimizations were carried out, focusing on a energetic comparison of extractive distillation processes using [EMIM][BF_4] and 1,2-ethanediol as entrainers, respectively. For approximately the same entrainer mass flows, the extractive distillation column of the [EMIM][BF_4]-process needs a heat input, which is considerably lower than that of the ethanediol-process. Since, for non-volatile entrainers such as [EMIM][BF_4] or hyperbranched polyglycerol, the entrainer regeneration can be realized not only by stripping but also by evaporation, drying or crystallization, further advantages in contrast to conventional extractive distillation processes are conceivable.

Future work will focus on developing a systematic approach, which allows for a problem-specific selection/tailoring of the most suitable ionic or hyperbranched entrainer. Furthermore, the influence of other IL and HyP on a variety of azeotropic systems will be studied so that g^E-models, a priori methods and equation of states can be tested and – if necessary – be modified in such a way, that they can be used for the complex selection process of entrainers.

NOMENCLATURE

List of Symbols

Latin letters

a,b,c,d,e,f	[-]	NRTL-model parameters in Aspen Plus
C_x	[-]	Parameter for calculation of c_p
D_x	[-]	Parameter for calculation of P^{LV}
G	[-]	Parameter of NRTL-model
Δg	[K]	Interaction parameter (NRTL-model)
g^E	[J/mol]	Excess Gibbs energy
K	[-]	Distribution coefficient
k	[J/K]	Boltzmann's constant
M	[kg/kmol]	Molecular weight
P	[Pa]	Pressure
S	[-]	Selectivity
T	[°C]	Temperature
w	[-]	Weight fraction
x	[-]	Liquid phase mol fraction
y	[-]	Vapor phase mol fraction

Greek letters

α	[-]	nonrandomness parameter (NRTL-model)
α_{ij}	[-]	Separation factor
β	[-]	Separation efficiency
γ	[-]	Activity coefficient
τ	[-]	Parameter of NRTL-model
φ	[-]	Fugacity coefficient

Subscripts

0	Pure substance
i	Component i
j	Component j

Superscripts

V	Vapor phase
L	Liquid phase

Abbreviations

DB	Degree of branching
DMF	Dimethylformamide
ED	1,2-Ethanediol
[EMIM][BF_4]	1-Ethyl-3-methylimidazolium tetrafluoroborate
EOS	Equation of state
GC	Gas chromatograph
HSGC	Headspace – gas chromatography
HyP	Hyperbranched polymers
IL	Ionic liquid(s)
LLE	Liquid-liquid equilibrium
Ma%, ma%	Mass percent
NMR	Nuclear magnetic resonance
NRTL	Non-random two liquid
PEG	Poly(ethylene glykol)
PG	Hyperbranched polyglycerol
SEC	Size exclusion chromatography
THF	Tetrahydrofuran
VLE	Vapor-liquid equilibrium

ACKNOWLEDGEMENTS

The authors thank Dr. H. Frey and Dipl.-Chem. H. Kautz for providing hyperbranched polyglycerol samples and Perstorp Speciality Chemicals AB for providing hyperbranched aliphatic polyesters. The authors gratefully acknowledge advisory information of Dr.-Ing. R. Hirsch regarding ASPEN PLUS®. We also would like to thank Dr.-Ing. D. Seifert for DSC-measurements, cand.-Ing. M. Buggert for his experimental assistance and Dipl.-Ing. O. Spuhl for modeling the VLE of ethanol–water–ethanediol using the PC SAFT equation of state.

REFERENCES

1. P. Walden; Bull. Acad. Imper. Sci. - St. Petersburg, 1800 (1914).
2. J. S. Wilkes, M. J. Zaworotko; Chem. Commun. 13 (1992) 965.
3. <http://www.solvent-innovation.de> [Accessed March 2002].
4. K. R. Seddon; Proc. of 5th International Conference on Molten Salt Chemistry and Technology, Molten Salt Forum 5-6 (1998) 53-62.
5. C. M. Gordon; Applied Catalysis A, General 222 (2001) 101-117.
6. M. Freemantle; Science/Technology., 78, 20 (May 2000) 37-50.
7. P. Wasserscheidt, W. Keim; Angew. Chem., 112 (2000), 3926-3945.
8. T. Welton; Chem. Rev., 99 (1999) 2071-2083.
9. P. Bonhôte, A. P. Dias, N. Papageorgiou, K. Kalyanasundaram; M. Grätzel; Inorg. Chem., 35 (1996) 1168-1178.
10. H. L. Ngo, K. LeCompte, L. Hargens, A. B. McEwen; Thermochimica Acta, 357-358 (2000) 97-102.
11. J. D. Holbrey, K. R. Seddon; J. Chem. Soc., Dalton Trans., (1999) 2133-2139.
12. J. D. Holbrey, K. R. Seddon; Clean Products and Processes 1 (1999) 223-236; Springer Verlag.
13. J. L. Anthony, E. Maginn, J. F. Brennecke; J. Phys. Chem. B (2001) in press.
14. D. S. H. Wong, J. P. Chen, J. M. Chang, C. H. Chou; Fluid Phase Equilibria 4954 (2002) 1-7.
15. S. S. Murugan, M. D. McKinley, R. H. Dubois, J. L. Atwood; J. Chem. Eng. Data, 45 (2000) 841-845.
16. A. E. Visser, R. P. Swatloski, S. T. Griffin, D. H. Hartman, R. D. Rogers; Sep. Sci. Technol., 36, 5&6, (2001) 785 – 804.
17. D. Swartling, L. Ray, S. Compon, D. Ensor; SAAS Bull. Biochem. Biotechnol., 13 (2000) 1-7.
18. L. A. Blanchard, J. F. Brennecke; Ind. Eng. Chem. Res., 40 (2001) 287-292.
19. F. Vögtle, Dendrimers, Top. Curr. Chem., 197, Berlin/Heidelberg, 1998.
20. M. Seiler, Chem. Eng. Technol., 25, 3 (2002) 237-253.
21. M.Seiler, W. Arlt, H. Kautz, H. Frey, Fluid Phase Equilib. (2002) in press.
22. K. Inoue, Prog. Polym. Sci., 25 (2000) 453-571.

23. W. Arlt, M. Seiler, G. Sadowski, H. Frey, H. Kautz (2001), DE Pat. No 10160518.8.

24. M. Seiler, D. Köhler, W. Arlt „Hyperbranched polymers – new classes of selective solvents for liquid-liquid extraction“, Fachausschußsitzungen on ‘Thermische Zerlegung, Adsorption und Extraktion’, Bingen/Rhein, Germany, 2002.

25. H. Hachenberg, K. Beringer, Die Headpsace-Gaschromatographie als Analysen- und Meßmethode, Vieweg Verlag, Braunschweig, 1996

26. G. Sadowski, L. V. Mokrushina, W. Arlt, Fluid Phase Equilib., 139 (1997) 391-403.

27. H. Kautz, A. Sunder and H. Frey, Macromol. Symp., 163 (2001) 67-74.

28. W. O. Pat. 93/17060, E. P. Pat. 0630389, U.S. Pat. 5418301 (1995) Perstorp AB (SE) (Inv.: Hult, A., Malmström, E., Johansson, M., Soerensen, K.).

29. A. Burgath, A. Sunder, H. Frey, Macromol. Chem. Phys., 201 (2000) 782-791.

30. <http://i-systems.dechema.de/detherm/>[Accessed March 2002].

31. A. M. Al-Amer, Ind. Eng. Chem. Res., 39 (2000) 3901-3906.

32. R. C. Pemberton, C. J. Mash, J. Chem. Thermodyn., 10 (1978) 867-888.

33. W. Arlt, M. Seiler, C. Jork, T. Schneider (2001), DE Pat. No 10114734.

34. W. Arlt, M. Seiler, C. Jork, T. Schneider (2001), DE Pat. No 10136614.

35. M. Seiler, D. Köhler, W. Arlt, Separation and Purification Technology (2002) in press.